Practical insights into ultrasound-assisted heterogeneous Fenton membrane reactors for water treatment

Yandi Lan, Christel Causserand, Laurie Barthe

Practical insights into ultrasound-assisted heterogeneous Fenton membrane reactors for water treatment

Yandi Lan, Christel Causserand, Laurie Barthe

Laboratoire de Génie Chimique, Université de Toulouse, CNRS, INPT, UPS, Toulouse, France

Abstract

Cavitation damage to membranes is a major barrier for developing an ultrasound (US)-assisted membrane water treatment process. In this study, US was integrated to a heterogeneous Fenton membrane reactor for the treatment of pharmaceutical-containing water with the aims of i) fouling control, ii) enhancement of heterogeneous Fenton oxidation. In order to prevent membrane damages due to cavitation, the stable and violent cavitation regions were identified by quantification and analysis of the cavitation activity axial along the ultrasound transducer via hydrophone measurements. Results showed the cavitation activities occur in both regions with US on, while the cavitation damage to membrane materials was only observed when membranes were placed in the violent cavitation region. On one hand, cracking and physical erosion of the surface were observed on membrane samples when exposed to violent cavitation. On the other hand, no such erosion occurred in stable cavitation regions, and membranes kept their mechanical, chemical and morphological properties, confirming that cavitation damage was controlled by placing membranes in the identified stable cavitation region. Based on these results, a heterogeneous Sono-Fenton membrane reactor was designed by placing a scalable hollow-fibre membrane module in the stable cavitation region. Within this reactor, the experiments confirmed that the oxidation of organics was enhanced thanks to the US assistance in the novel designed heterogeneous Sono-Fenton membrane reactor. However, this study also showed that US accelerated membrane ageing and zeolite-catalysts erosion, leading to more severe fouling. Overall, this paper introduces a method to control the cavitation damage to membranes and discusses the issues in US-assisted membrane systems with practical insights.

Keywords: Ultrasound, Microfiltration, Cavitation damage, Ultrasonic fouling control, Heterogeneous Sono-Fenton oxidation

1. Introduction

The production and demand of pharmaceuticals has dramatically increased for high economic growth and better human health [1]. However, the discharge of pharmaceuticals contained wastewater, from all kind of sources such as the pharmaceutical industry and hospital effluents, has become a major challenge to the sustainability of the aquatic system: most pharmaceuticals are partially- or non-biodegradable and resistant to the conventional activated sludge process of a wastewater treatment plant (WWTP), releasing into the environment [2]. These refractory pharmaceuticals accumulate in the aquatic ecosystems and pose significant threats to the ecosystem's sustainability and drinking-water safety [3,4]. It is therefore crucial to develop new and advanced treatment systems. In particular, integrated treatment systems combining several techniques have recently become a very interesting approach, providing additional options for treatments of harsh wastewater or high discharge standard [5–10].

Membrane-based oxidation processes are increasingly attracting attention for water treatment as the integration of membrane filtration and advanced oxidation processes efficiently remove and eliminate refractory pollutants [5,7,11–14]. In these processes, the role of membranes can be applied to separate and concentrate pollutants [7,11,12] or complete an oxidation reactor by retention and reuse of the catalysts [5,14]. However, the process efficiency is limited by the membrane fouling induced by the components in wastewater matrix or catalysts in oxidation reactors. To tackle fouling issues, the integration of ultrasound (US) with membrane filtration has been widely studied during the last two decades [15–20]. US enables to detach or loosen deposits/particles from membrane surfaces by cavitation mechanism (i.e., microjets) and transport foulants away from the surface by acoustic streaming [19]. Indeed, US enables to promote both physical and chemical processes [21,22]. Besides fouling control, US furthermore promisingly improves oxidation efficiency in a membrane-based oxidation process [10,23], for example, US enhanced heterogeneous Fenton oxidation (Sono-Fenton) in multiple functions [8,24–26]. US improving Fe^{2+} regeneration and subsequent formation of radicals in the heterogeneous Fenton reactor has been proven. Moreover, US assisted the mineralization of organic pollutants. It was found that the mineralization degree of phenol by heterogeneous Fenton oxidation was significantly enhanced with up to 90% of TOC removal after US irradiation [27]. This enhancement of the mineralization of organic pollutants can be associated to US preventing from the catalyst deactivation, the formation of other reactive oxidant species, and/or thermal cleavage of volatile compounds, contributing to the acoustic cavitation which gives rise to extreme conditions inside and around the collapsing bubble - up

to 5000 K and 500 bar. The cavitation also contributes to the increase of accessible surface of catalysts by its mechanical effects.

The cavitation activities induced by US irradiation in the water potentially benefits both membrane fouling control and oxidation efficiency. However, the cavitation damage to membrane materials is a major concern for the integration of US into membrane-based processes. It was widely reported that cavitation and bubble implosion may induce physical and chemical erosion of membrane materials [28–31]. Indeed the damaging effects of US are highly related to the cavitation type and intensity[32]. During acoustic cavitation, gas bubbles appear due to acoustic waves. Depending on the bubble size and local acoustic pressure, the oscillation of a bubble is variable. Schematically, some bubbles violently collapse (transient cavitation), generating a very strong shock wave, followed by the production of •OH radicals responsible for mechanical and chemical damage to materials. Other types of bubbles slightly oscillate and are more stable with a relatively long lifetime (stable cavitation) [33]. This latter type of cavitation is less active and so less destructive to materials. Therefore, the cavitation damage to membranes can be potentially controlled by identifying the cavitation intensity and minimising the effects of violent cavitation activity.

To promote US assisted membranes and advanced oxidation processes for water treatment, the present study integrated sonication with the heterogeneous Fenton membrane reactor which was investigated in our previous study [14]. A heterogeneous Sono-Fenton membrane reactor (HSoFM) was then developed for the degradation of pharmaceuticals in an aqueous solution. The oxidation ability of this process is attributed to highly reactive hydroxyl radicals (•OH) generated from Fenton-like reactions involving hydrogen peroxide as the oxidant and iron-containing micro-sized zeolites as catalysts [34]. The role of membrane filtration in the HSoFM reactor is to retain the zeolite catalysts in the effluent compartment during the continuous water treatment, overcoming the issue of difficult iron recovery in the Fenton oxidation process [35]. The further integration of the sonication in this process is of great interest to control membrane fouling induced by the zeolite catalysts and to enhance the degradation of pharmaceuticals.

In this present paper, the practical aspects of the coupling of US with membranes and advanced oxidation processes for water treatment have been discussed. Firstly, a stable cavitation strategy for controlling cavitation damage to membrane materials was investigated. Secondly, the violent and stable cavitation regions were identified by quantification and analysis of the cavitation activity axial along with an ultrasound transducer via hydrophone

measurements. The control of cavitation damage to membranes in the stable cavitation region was then verified, following the analysis of the role of US on membrane ageing in a Sono-Fenton aggressive media. Moreover, since the chemical effects of ultrasound on membrane are rarely investigated in the literature [36], the impact of both the chemical and physical effects will be discussed in this study. The model system, a bench-scale HSoFM reactor with a scalable hollow-fibre membrane module, was then designed by placing the membrane module in a stable cavitation region. Two potential benefits of US in water treatment processes, fouling control and oxidation enhancement, were then evaluated in the HSoFM reactor.

2. Materials and methods

2.1 Chemicals and membrane

All aqueous solutions were prepared using deionized (DI) water generated by a PURELAB maxima system (ELGA labwater's, UK). Ibuprofen (IBP, $C_{13}H_{18}O_2$, purity 99.99%) was purchased from BASF Corporation and used as received. Hydrogen peroxide (H_2O_2, 30% w/w), sulphuric acid (1 mol/L), titanium tetrachloride solution (0.09 mol/L in 20% HCl) for H_2O_2 concentration analysis, monopotassium phosphate (KH_2PO_4) and sodium phosphate dibasic dehydrate (Na_2HPO_4,$2H_2O$) for preparing the buffer solution were purchased from Sigma-Aldrich. A commercial iron-containing zeolite of ZSM-5 structure (provided by Clariant^{TM}) was used as Fenton's reagents. This zeolite exhibited a Si/Al ratio of 13 and an iron content of 3.5 wt%. The average particle size of this catalyst is approximately 8 μm [35].

MF0808XS Polysulfone/Polyvinylpyrrolidone (PSU/PVP) hollow-fibre membrane module (provided by Polymem^{TM}) was tested. PVP was blended (5%, w/w) into the PSU matrix to increase the hydrophilicity of the membranes. The membrane pore size was 0.1 μm (microfiltration membrane). In this study, membrane filtration was only intended to maintain the catalyst (approximately 8 μm) in the oxidation reactor during the continuous treatment rather than to selectively reject the pharmaceutical and by-products. The membrane module for the HSoFM reactor contained 200 fibres. Its total active membrane surface was approximately 0.07 m^2.

2.2 Cavitation activity analysis method

2.2.1 Cavitation activity and acoustic pressure

The aim of cavitation activity analysis was to estimate the intensity of axial cavitation activity along the US transducer. In the region where the major group of cavitation bubbles

was transient, the cavitation activity was intensive and violent. The violent collapse of (transient) cavitation bubbles most likely led to membrane erosion. Conversely, where the dominate cavitation bubbles was relatively stable (or long lifetime), the cavitation activity was considered stable and expectedly less destructive to membrane materials.

The intensity of cavitation activity can be related to the spectral components of the acoustic wave. The US spectrum includes a ray at the fundamental frequency f (emitted by the ultrasonic generator), possibly harmonics of this fundamental frequency (k.f), sub-harmonics (f/n) and ultra-harmonics (kf/n). Between all the rays there is a broadband noise. It was proposed that the fundamental frequency is associated with violent collapses of cavitation bubbles (potentially transient cavitation) that lead to mechanical and chemical damage to membranes. Conversely, harmonics induce a relatively long lifetime of the cavitation bubble.

Indeed, the intensity of the cavitation activities is highly dependent on the acoustic pressure [37]. For this reason, the cavitation activity can be estimated by measuring the acoustic pressure by means of a hydrophone (section 2.2.2). The hydrophone determines the frequency band for the majority of the signal power [38].

Therefore, by analysing the acoustic pressure axial along US transducer, the acoustic cavitation, due to the fundamental frequency, can be identified from the total US power. A stable cavitation region is identified where the majority of the cavitation bubbles are relatively stable. Conversely, in a violent cavitation region, the cavitation activities are violent and intense. In the stable cavitation region, the cavitation activities expectedly remain but intensive cavitation due to the fundamental frequency is minimized.

2.2.2 Acoustic pressure measurements with hydrophone and data analysis

The acoustic pressure measurements were performed using a hydrophone (model 8103) provided by Brüel & Kjær. The piezoelectric ceramic was encapsulated in a rubber cylinder 3 cm long and 0.7 cm in diameter. It was calibrated by the manufacturer who provided the evolution of the sensitivity in volts versus the acoustic frequency. This calibration curve relates the amplitude of the acoustic pressure to which the sensor is subjected to the resulting electric charge.

The measurement system then comprises three devices provided by Brüel & Kjær: an amplifier (model 1704) intended to simulate an infinite input impedance and whose gain is set to the unit value, a signal converter (model 2647 A) connected upstream of the amplifier 1704, and finally a load attenuator (model WB0779) connected to the hydrophone to remain in the voltage range compatible with the amplifier 1704 and thus avoid saturation at very high

acoustic pressures. At 20 kHz, this setup has a resulting sensitivity of 0.896 V/bar. It should be noted that this configuration had a cutoff frequency located at 50 kHz.

For data acquisition, the measurement system was connected to a digital oscilloscope (Pico Technology). This device makes it possible to measure and digitize the output voltage of the measuring device so a computer can register it. The whole measurement system involved in this study is represented in Figure 1.

The signal is processed with MATLAB software. After pretreatment of the signal, a spectral analysis was performed by Discrete Fourier Transform (DFT). The data processing is already detailed in a previous article [38]. Thus, a spectrum was obtained which determines the frequency bands where there is the majority of the power contained in the signal. It is then possible to determine the contribution to the total US power of the different elements of the spectrum (fundamental frequency, harmonics and broadband noise) by calculating the RMS (Root Mean Square value) pressure. According to the discussion in section 2.1, the RMS acoustic pressure contributions to the total US power and to the fundamental frequency were determined and analyzed to estimate the stable and violent cavitation regions axial along the ultrasonic probe.

2.3 Experimental set-up and protocol

2.3.1 Ultrasound generator and identification of the stable cavitation region

The ultrasound generator (SinapTec NexTgen Inside 500), connected with a Cup-Horn type transducer, was used for both the membrane stability tests set-up and HSoFM reactors. The operating ultrasound frequency is 20 kHz, which is commonly used for the integration of membrane-based processes since lower frequencies had higher cleaning efficiencies than higher frequencies [19]. The US power is fixed at 50 W because previous studies determined that membrane erosion was insignificant for US power less than 60 W [31].

To analyse cavitation activity axial along the US transducer, the acoustic pressure (section 2.2) was measured every 0.5 cm along US transducer using the hydrophone in a water-filled glassware. The stable and violent cavitation regions were estimated by quantification and analysis of acoustic pressure due to fundamental frequency of the total US power.

2.3.2 Membrane stability and ageing tests under US

The membrane stability under US was measured in a 1L jacketed thermostat glassware shown in Figure 2. The US transducer was located at the bottom of the glass reactor and membranes were fixed in a frame. By moving this frame up or down, the distance between membranes and the US transducer could be adjusted from 1.5 to 4 cm. This axial distance between membranes and the transducer tip is referred to as tip height. By adjusting the tip height, membranes can be exposed to identified stable or violent cavitation region.

For US exposure, the PSU/PVP membranes were immersed in DI water in the glassware. The tests were conducted for 10 hours under continuous 50 W US power by placing membranes in both stable and violent cavitation regions. Then the membranes were sampled and characterized.

Furthermore, to understand the effect of US on membrane ageing while exposed to oxidative media, PSU/PVP membranes were immersed into a heterogeneous Fenton reactive suspension containing 4.8 g L^{-1} of ZSM-5 zeolite and 6.4 mM H_2O_2 under stable cavitation. The concentration of catalysts and H_2O_2 was chosen according to selected conditions in a previous study on the heterogeneous Fenton membrane reactor [14]. The H_2O_2 concentration in the suspension was maintained at 6.4mM by continuous H_2O_2 injection using a syringe pump (Harvard PHD 2000). The US power was maintained at 50 W. For comparison, other groups of PSU/PVP membranes were submerged into Fenton reactive suspension with the same concentration of ZSM-5 zeolite catalyst and H_2O_2 under silent conditions. All the soaking tests were conducted for 30 hours. Membrane samples were taken periodically during the experiment for analysis.

2.3.3 Heterogeneous Sono-Fenton hollow-fibre membrane reactor

The HSoFM reactor was designed by placing the membrane module in the identified stable cavitation region for the control of cavitation damage (Figure S1 in supplementary information). The experimental solution was introduced in a 6.5 L thermo-regulated glass reactor. The membrane module reactor retains the catalyst in the glass reactor. The filtrations were performed in the outside-in filtration mode. The permeate was recycled back into the reactor to simulate a continuous process from a hydrodynamic point of view. The US transducer was located on the side wall of the reactor within the designed distance to the membrane module with on and off options.

The water treatment performance of HSoFM reactor was assessed by the degradation of the pharmaceutical solution. Ibuprofen (IBP), a widely used drug, was selected as the target pollutant for the reactor assessment, because it was found in effluents from various wastewater treatment plants and groundwater up to 95 µg/L [39]. IBP was dissolved in deionized water with an initial concentration of 20 mg L^{-1}. The stoichiometric amount of H_2O_2 (6.4 mM) was applied twice to avoid extensive scavenging of hydroxyl radicals. For effective production of hydroxyl radicals, the [H_2O_2]/[Fe] molar ratio was maintained at 10, and the catalyst concentration at 4.8 g/L. The concentration of H_2O_2 was maintained at 6.4mM due to its continuous injection using a syringe pump (Harvard PHD 2000) during oxidation. The water treatment experiments were conducted at a controlled temperature of 25 ± 2 °C. The rotation rate of the stirrer inside the reactor was 300 rpm.

In this preliminary test of HSoFM reactor, the objective was to understand the membrane fouling phenomenon and Fenton oxidation under sonication. Therefore, the water treatment process was conducted in two stages.

Stage one with US off. Filtration flux was maintained at 30 L h^{-1} m^{-2} for fouling development with US off and the variation of transmembrane pressure was monitored during the process. The filtration was performed at 30 L h^{-1} m^{-2} because this flux value was above the critical flux value (flux below which a decline of flux over time, due to irreversible fouling, does not occur, and above which irreversible fouling is observed [14]). Oxidation was started by injecting H_2O_2, when the adsorption of IBP by catalysts and membranes had reached equilibrium.

Stage two with US on. Filtration and oxidation were conducted following the same protocol as in stage one whilst US was switched on in this stage.

Since the HSoFM reactor is a constant permeate flux system, the development of fouling causes the increase in transmembrane pressure (TMP). In these two stages, transmembrane pressure was monitored to investigate fouling development. Solution samples were taken at regular intervals in the reactor for analysis and immediately treated by phosphate buffer (a mixture of KH_2PO_4 0.05M and $Na2HPO_4 \cdot 2H_2O$ 0.05 M) to reach a neutral pH after the removal of catalysts using a 0.45 µm RC syringe filter to stop the oxidation reaction.

2.4 Analysis

2.4.1 Solution analysis

To evaluate the water treatment efficiency, the total organic carbon (TOC) of solution samples from the reactor was analysed. The TOC value was calculated from the difference between Total Carbon (TC) and Inorganic Carbon (IC), measured by a TOC-L analyser (Shimadzu). The TC of all samples was measured three times and the coefficient of variation was less than 2 %. Calibration curves were established using commercially available standard solutions (Shimadzu).

2.4.2 Membrane characterization

SEM-EDX Scanning electron microscope with energy-dispersive X-ray spectroscopy. Morphology and elemental information on the membrane surface were examined with a SEM (Hitachi Tabletop Microscope TM-1000) interfaced with an EDX spectroscopy system (Thermo-Fisher). Samples were coated with a thin layer of gold before SEM analysis for better contrast. EDX analyses were carried out at the same time. EDX measurements were performed at different locations of the membrane surface to obtain a comprehensive elemental composition.

ATR-FTIR Attenuated Total Reflection-Fourier Transform InfraRed spectroscopy was obtained with a Thermo-Nicolet Nexus 670 apparatus (USA). The sample was placed on diamond crystal substrates and the analytical depth was approximately 2 μm. Membrane samples after soaking in the reactive medium were firstly dried at 40 °C for 48 h. Then they were examined using ATR-FTIR spectra to identify chemical membrane changes. All the recorded PSU/PVP IR spectra were corrected by adjusting the 1587 cm^{-1} band to an arbitrary chosen absorbance value of 1. This band corresponds to an aromatic in-plane ring bend stretching vibration of the PSU and considered to be invariable during membrane degradation [14]. The corrected absorbance is mentioned as relative absorbance. To facilitate the reader's understanding, when monitoring changes of specific IR bands upon degradation, normalization by dividing the relative absorbance by the one of the pristine membranes was performed.

Tensile testing Tensile tests were performed to obtain the stress-strain curve, reflexing membrane's mechanical property. The measurements were performed on wet membranes using an INSTRON 4281 series tensile apparatus. Tailor-made grips for the hollow-fibre geometry were fitted to the device to avoid stress concentration. The initial distance between grips was fixed at 50mm and samples were extended at a constant elongation rate of 100

mm/min. Ultimate elongation at breakpoint was calculated from the experimental stress-strain curves. A set of five samples were analysed and averaged for each tested condition.

3. Results and discussion

3.1 Determination of the stable cavitation region

This section aims to determine a stable cavitation region where the cavitation bubbles are relatively stable (or long lifetime) and less violent to membrane materials. As discussed in section 2.2.1, the fundamental frequency is usually associated with violent collapses of cavitation bubbles, while harmonics induce the relatively long lifetime cavitation bubble [38]. Therefore, by means of a hydrophone (section 2.2), the fundamental frequency from the ultrasonic spectrum was identified and its associated cavitation activity characterized by the RMS acoustic pressure was determined. The stable cavitation region was identified. In this region, cavitation activities (by RMS acoustic pressure) remain, but RMS acoustic pressure associated to the fundamental frequency are minimized.

To identify the frequencies of the ultrasonic wave, the time-frequency signal was measured by a hydrophone, followed by a Fourier transform spectral analysis. The spectrum obtained from the signal measurement at 1.5 cm tip height is presented in Figure 3a. The frequencies were identified by indicating their amplitude. Two peaks were detected in Figure 3a, corresponding to the fundamental frequency (20 kHz) and the first harmonic (40 kHz) with the 50 kHz frequency cut-off of the measuring system.

Figure 3b shows the RMS acoustic pressure of fundamental frequency (20 kHz) and total power as a function of the axial distance to the transducer tip (referred to as tip height). Each value in the graph is obtained from an average of 32 spectra. One can observe that the RMS acoustic pressure of fundamental frequency dramatically decreased from 0.2 bar with the increase in tip height until reached the lowest value (0.02 bar) at 3.5 cm. On the other hand, RMS acoustic pressure of total power was 0.28 bar at the initial point (1.5 cm tip height). After approximately 50% decline, its value relatively stabilized at around 0.15 bar from 2 cm to 4 cm tip height. Figure 3c highlights the ratio of RMS acoustic pressure of fundamental frequency to total power. It was found that the percentage of RMS acoustic pressure of fundamental frequency decreases from 1.5 cm to 3.5 cm tip heigh then increases.

The estimation of the intensity of cavitation activity depends on both the magnitude of RMS acoustic pressure induced by the fundamental frequency as well as its percentage in the RMS

acoustic pressure of total US power. Therefore, for a tip height of 1.5 cm, the RMS acoustic pressure induced by the fundamental frequency is high (0.2 bar) and accounts for 73% of the RMS acoustic pressure of total power. The violent collapse of the cavitation bubbles associated with fundamental frequency likely occurred there, thus this region was referred as 'violent cavitation'. In contrast, at 3.5 cm tip height, the RMS acoustic pressure of the fundamental frequency is much lower (0.02 bar, 10 % of that at 1.5 cm) and only takes account for the 23% of RMS acoustic pressure of total power. Considering the remaining 0.12 bar (~40 % of that at 1.5 cm) of the RMS acoustic pressure induced by total power, this region remains the cavitation activity, whilst most of the cavitation bubbles induced by the harmonics should be less violent to membranes. This region was referred to as a "stable cavitation", where membrane rupture by US expectedly was minimized whist the cavitation-cleaning capacity of US remains.

3.2 Membrane stability in water under violent and stable cavitation

In this section, membrane stability was compared in the determined stable cavitation region and in the violent cavitation region (3.5 cm and 1.5 cm to transducer tip, respectively). In this comparison objective, membranes were placed in the test system (section 2.3.2) filled with water. The surface morphology, as well as mechanical and chemical properties of membranes were monitored.

Cracks were observed on the membranes exposed to violent cavitation for 10 h. From SEM images in Figure 4b, irregular-section cracks were found. The surface of the membranes was eroded (Figure 4d), as demonstrated by the disappearance of the membrane selective skin by comparing to the surface of the pristine membrane (Figure 4a). On the other hand, no such crack and no significant changes in membrane micro-surface morphology were found on the membranes exposed to stable cavitation (Figure 4c). Moreover, the stress-strain curve obtained by tensile tests on membrane samples subjected to stable cavitation is presented in Figure S2 in supplementary information. The curve shapes of these membranes remain the same as that of pristine membranes, indicating that membranes mechanical strength is maintained.

The chemical changes of membranes in stable and violent cavitation regions were analysed by EDX and FTIR. It's worth noting that the PSU/PVP membranes used in this study were made from PSU blended with 5% PVP. The fraction of PVP on the membrane material can be monitored by the N/S atomic ratio, because repeat units of PSU and PVP carry only one sulphur atom (S) and one nitrogen atom (N), respectively. From the EDX analysis, the N/S atomic ratio of membranes submitted to stable cavitation maintained the same value of the

pristine membrane N/S atomic ration (4.53 ± 0.6), whilst the ratio decreased from 4.53 ± 0.6 to 1.88 ± 0.4 upon exposure to violent cavitation. Moreover, according to FTIR analysis (Figure S3 in supplementary information) of membranes exposed to both violent and stable cavitations, no new absorbance band appears in their FTIR spectra comparing to that of the pristine membrane. The band at 1674 cm^{-1} corresponding to the stretching vibration of the amide unit of the PVP, and the one at 1145 cm^{-1} associated with symmetric SO_2 stretching vibration of PSU [40] were analysed. The ratio of these two absorbance's (-N- of PVP / SO2 of PSU) on membranes submitted to violent cavitation is around 0.08, which is below the ratio obtained for pristine membranes (0.18), and for membranes exposed to stable cavitation (0.16). These results are in accordance with the EDX analysis. They enable the conclusion that, under violent cavitation, the PVP fraction on the membrane material decreases mainly by PVP dislodgement from the membrane rather than by its chemical degradation (no new band observed by FTIR). This is in accordance with MEB observations: the membranes exposed to violent cavitation dominantly suffered from physical erosion under 50 W ultrasonic irradiation when this erosion is negligible for membranes submitted to stable cavitation

These results confirmed that the exposure of membranes to stable cavitation effectively controls their cavitation damage. In these conditions, membranes maintained their mechanical and chemical properties as well as their surface structure. Exposing membranes to violent cavitation, although with a relatively low US power of 50W, led to severe damage, or even cracking.

3.3 Role of US on membrane ageing during exposure to oxidative media

Membrane ageing, the degradation of the membrane over time, was evaluated during exposure to oxidative media, resulting in performance decline or complete membrane failure [41,42]. Therefore, besides the control of cavitation damage to membranes, it is important to understand the membrane ageing process in the heterogeneous Sono-Fenton reactor. With this aim, PSU/PVP hollow-fibre membranes were placed under stable cavitation and submerged in Fenton reactive medium (4.8 g L^{-1} catalyst and 6.4 mM H_2O_2). To identify the role of US on membrane ageing, another group of membranes was soaked in a Fenton reactive medium under silent conditions (US off). Changes in mechanical and chemical properties of the membrane material were then monitored.

Mechanical properties of membranes in Sono-Fenton and Fenton media were monitored as a macroscale view of changes in material performances. By comparing the stress-strain curves

of membranes sampling at different exposure times, it was found that the shapes of the elastic domain and early stages of the plastic domain were generally unchanged (results not shown), while the ultimate elongation value (at break) appeared to be affected. The ultimate elongation, therefore, was the most sensitive parameter compared, for example, to Young's Modulus. For this reason, the ultimate elongation was presented to demonstrate the change in mechanical properties of the membranes. The variation of ultimate elongation of membranes over exposure time is shown in Figure 5a. One can observe that, without US, ultimate elongation of membranes remained constant. On the other hand, when membranes were submitted to US, their ultimate elongation slightly decreased, before reaching a plateau at around 80% of the initial value after a 20-hour exposure. At the same time, SEM images of these last membrane samples after a 30-hour exposure presented a similar surface to that of the pristine membrane, indicating no significant change in membrane surface morphology (Figure S4 in supplementary information).

The change in chemical properties of 30h-aged membranes was then investigated by FTIR and EDX analysis. FTIR spectra of PSU/PVP membranes after 30-hour exposure to Fenton (US off) and Sono-Fenton (under stable cavitation) were presented in Figure 5c. The major distinction among the spectra appeared from 1700 to 1630 cm^{-1}. The intensity of the IR band at 1674 cm^{-1} characteristic of PVP, decreased in samples submitted to Sono-Fenton medium compared to the pristine membranes. At the same time, a sharp absorbance peak appeared at 1735cm^{-1}, associated with the formation of non-cyclic imide groups, characteristic of degradation products of PVP resulting from hydroxyl radical attack [43]. On one hand, these results revealed that the chain scission of PVP occurred when membranes are submitted to Sono-Fenton conditions. Furthermore, the absorbance intensity at 1735 cm^{-1} increased with exposure time and then stabilized after a 20-hour exposure to Sono-Fenton conditions (panel of Figure 5c). It is likely that the PVP chain scission developed more quickly at the early stage of exposure, then stabilised. On the other hand, previous studies [14] showed that the chain scission of PSU evidenced with absorbance peaks at 1638 cm^{-1}, caused a dramatic decrease in membrane mechanical properties. Herein, no such peaks were observed in the FTIR spectra of aged membranes. These results show that US induced chain scission of the PVP additive when the PSU is not oxidated. The chemical properties stabilization after a 20-hour exposure (stabilized PVP chain scission and absence of PSU chain scission) is in accordance with the behaviour in mechanical properties: decrease in ultimate elongation of aged membranes, followed by stabilisation after a 20-hour exposure (Figure 5a).

As discussed in section 3.2, the N/S atomic ratio from the EDX analysis represents the fraction of PVP on the membrane surface. Figure 5b compares the N/S atomic ratio of pristine membrane and samples exposed to Fenton (US off, 10, 30-hour exposure) and Sono-Fenton media (5, 10, 20, 30-hour exposure). One can find after a 5-hour exposure to Sono-Fenton, the N/S atomic ratio on the surface of membranes decreases to 75% of the pristine value. This ratio was then maintained until the end of the experimental period (30-hour exposure). That is to say, the release of PVP additive from the membranes mainly occurred at the early stage of exposure. Combining the FTIR analysis (spectra shown in Figure 5c), it was found that the membrane ageing in Sono-Fenton began with the release of a certain amount (~25%) of PVP additive at the early stage (<5-hour exposure). After, the further membrane ageing involved the chain scission of PVP (chemical properties change) until reaching stabilisation after a 20-hour exposure.

By comparing the FTIR spectra and N/S atomic ratio of aged membranes in Fenton medium (US off), no significant change in IR absorbance was observed and the N/S atomic ratio kept 90% of that of pristine membranes. These results indicated that membrane ageing was accelerated under US radiation. Although the acceleration of membrane ageing by US radiation is likely to a controllable degree: membranes properties stabilisation and no significant degradation of backbone material, one can suggest the application of a pulsed mode ultrasound, reducing the US exposure time, in a US-assisted membrane process for a sustainable system.

3.4 HSoFM reactor design and preliminary test for water treatment

Placement of membranes in a stable cavitation region is evident in order to prevent cavitation damage of membranes while keeping the cavitation-cleaning capacity of US. According to the study in section 3.1, a 6.5L bench-scale HSoFM reactor (Figure S1 in supplementary information) was designed, where a scalable hollow-fibre membrane module was placed in a stable cavitation region (~3.5 cm to the transducer tip). In this preliminary test of HSoFM reactor, the objective was to evaluate over time the oxidation of organic pollutants and the evolution of membrane fouling when US are applied. Therefore, the heterogeneous Fenton oxidation was conducted in the reactor in two stages (section 2.3.3): stage one under silent conditions (with US off) to preform fouling induced by zeolite catalysts; stage two with US on for treatment of membrane fouling.

The HSoFM reactor was filled with 4.8 g L^{-1} zeolite catalysts. The oxidation of ibuprofen in water was started by continuous injection of H_2O_2. Figure 6a shows that the TOC of the solution in the reactor decreased from the beginning of oxidation and reached a plateau

from 180 min at stage one (US off). No significant decrease of TOC was found from 180 min to 300 min of oxidation time. These results indicate that the heterogeneous Fenton oxidation (US off) contributed little to oxidate organic pollutants until total mineralisation, which is in accordance with other studies [44,45]. Since the FeZSM-5 catalysts are stable over several sequential uses in oxidation reactions [44], the plateau of TOC from 180 min oxidation is likely due to the formation of refractory oxidation intermediates. With US on (Sono-Fenton oxidation, stage two), the TOC value of the solution in the reactor decreased again in 40 min with statistical significance ($p<0.05$), confirming that US integration enhanced the Fenton oxidation in the HSoFM reactor. According to previous studies [8,27], the enhancement of mineralization degree by US (TOC decrease) is probably attributed to 1) additional powerful oxidants, •OH radicals, generated by water sonolysis (US on), 2) US improving Fe^{2+} regeneration and subsequent formation of radicals.

For the fouling control aspect, since the HSoFM reactor is a constant permeate flux system, the development of fouling causes an increase in transmembrane pressure (TMP). A higher increase rate of TMP reflected a faster fouling rate. Figure 6b presents the evolution of TMP and the permeate flux from the beginning of oxidation treatment. At stage one (US off), the operating flux is constant at 30 L h^{-1} m^{-2}. According to the value of critical flux for irreversible fouling in the HSoFM reactor (23 L h^{-1} m^{-2}), the operating flux is above this threshold value [14]. The fouling induced by the catalysts is then expected to be irreversible, which means the foulants persisted on the membrane even if the TMP decreases [14]. From Figure 6b, the TMP increased due to the fouling occurrence. During a 3-hour filtration (US off), the irreversible fouling was further developed with an average rate of 8.7×10^{-5} bar min^{-1}. Thereafter, the experiment turned into stage two with US on. The TMP unexpectedly increased faster than for stage one with an average rate of 2.3×10^{-4} bar min^{-1}. Rather than mitigating fouling, applying US likely led to a more rapid formation of fouling. To understand this phenomenon, membrane samples were taken from the module and SEM analysis were performed. From the SEM images in Figure 6c, one can observe that many fine catalyst fragments were firmly adhesive to the membrane surface, blocking the membrane pores. The reduction of catalyst size under US was confirmed by particle-size distribution test (Figure S5 in supplementary information). The size decreases from D90=13.5 µm for initial zeolite catalysts to D90=11.4 µm and 6.51 µm for catalysts after 10 and 30-hour exposure to US respectively. Hence, it appears that the catalysts were eroded under US, the fine catalyst fragments leading to severe membrane fouling. Similar phenomena were reported in a study

using US control of fouling by sludge flocs. US radiation cracking the sludge flocs caused the deterioration of membrane fouling condition [16]. In their study, the performance of US for fouling control was improved by optimising the radiation length and by integrating a flush of the membrane in the process. Therefore, applying the pulse-mode US (reducing the US exposure time), and/or integrating backwashing could be some solutions to this issue. It's worth noting that the pulse-mode US also benefits membrane stability under US as discussed before. For these reasons it can be suggested that pulse-mode radiation be used in a US-assisted membrane and oxidation process and optimize the HSoFM reactor with a pulse-mode US in further study.

4. Conclusion

This study discussed the practical aspects of the integration of ultrasound with membrane and advanced oxidation process for water treatment. A model system integrating ultrasound with heterogeneous Fenton membrane reactor was designed for pharmaceutical oxidation where a scalable hollow-fibre membrane module was applied. US was integrated in the system to potentially enhance heterogeneous Fenton oxidation and control fouling induced by zeolite catalysts.

A stable cavitation strategy was first investigated for the control of cavitation damage to membranes, a major concern for US-assisted membrane-based processes. The intensity of cavitation activity axial along ultrasound transducer was quantified by hydrophone measurements and spectrally analysed. The stable cavitation located at 3.5 cm to the transducer tips was identified, where cavitation activities were in a minority generated by harmonics and so less violent to membrane materials. After tests of membrane stability in both stable and violent cavitation regions confirmed that membranes placed in a stable cavitation region kept their mechanical and chemical properties and surface morphology. Exposing membranes to the violent cavitation region, albeit with a relatively low US power of 50W, led to severe physical damage of the membranes and even cracking.

Considering the sustainable aspect of the US-membrane system, the role of US on membrane ageing was then studied in a stable cavitation region. US radiation was found to accelerate membrane ageing in the oxidative Sono-Fenton medium, but likely in a controllable degree. On one hand, the membrane ageing involved the decrease in PVP additive content (5%

in the virgin membrane material) partly by dislodgment from the membrane structure, and partly by chain scission. However, this PVP degradation reached a stable state under the experimental period. On the other hand, absence of degradation of the backbone material (PSU) of membranes was observed.

A heterogeneous Sono-Fenton membrane (HSoFM) reactor was designed by placing a hollow-fibre membrane module in a stable cavitation region for bench-scale testing. The preliminary tests confirmed that US integration enhanced the heterogeneous Fenton oxidation of organic pollutants in the HSoFM reactor: TOC reduction by Fenton oxidation in the reactor reached a plateau, but, when US applied, TOC value decreased again. However, US unexpectedly eroded the catalysts and the fine catalyst fragments caused severe fouling. A pulsed mode US was proposed for further optimisation of HSoFM reactor and control of the membrane ageing under US.

Acknowledgment

This work was supported by ANR (French National Research Agency) through ANR project "SOFENcoMEM" (ANR 14 CE04 0006).

Reference

[1] Treatment of wastewater containing pharmaceuticals: biological treatment, Curr. Dev. Biotechnol. Bioeng. (2020) 463–520. https://doi.org/10.1016/B978-0-12-819722-6.00013-4.

[2] S. Rodriguez-Mozaz, S. Chamorro, E. Marti, B. Huerta, M. Gros, A. Sànchez-Melsió, C.M. Borrego, D. Barceló, J.L. Balcázar, Occurrence of antibiotics and antibiotic resistance genes in hospital and urban wastewaters and their impact on the receiving river, Water Res. 69 (2015) 234–242. https://doi.org/10.1016/j.watres.2014.11.021.

[3] W.C. Li, Occurrence, sources, and fate of pharmaceuticals in aquatic environment and soil, Environ. Pollut. 187 (2014) 193–201. https://doi.org/10.1016/j.envpol.2014.01.015.

[4] G.M. Bruce, R.C. Pleus, S.A. Snyder, Toxicological Relevance of Pharmaceuticals in Drinking Water, Environ. Sci. Technol. 44 (2010) 5619–5626. https://doi.org/10.1021/es1004895.

[5] Y.-Y. Zhang, C. He, V.-K. Sharma, X.-Z. Li, S.-H. Tian, Y. Xiong, A new reactor coupling heterogeneous Fenton-like catalytic oxidation with membrane separation for degradation of organic pollutants, J. Chem. Technol. Biotechnol. 86 (2011) 1488–1494. https://doi.org/10.1002/jctb.2656.

[6] S. Arefi-Oskoui, A. Khataee, M. Safarpour, Y. Orooji, V. Vatanpour, A review on the applications of ultrasonic technology in membrane bioreactors, Ultrason. Sonochem. 58 (2019) 104633. https://doi.org/10.1016/j.ultsonch.2019.104633.

[7] Y. Lan, C. Coetsier, C. Causserand, K. Groenen Serrano, An experimental and modelling study of the electrochemical oxidation of pharmaceuticals using a boron-doped diamond anode, Chem. Eng. J. 333 (2018) 486–494. https://doi.org/10.1016/j.cej.2017.09.164.
[8] M. Gągol, A. Przyjazny, G. Boczkaj, Wastewater treatment by means of advanced oxidation processes based on cavitation – A review, Chem. Eng. J. 338 (2018) 599–627. https://doi.org/10.1016/j.cej.2018.01.049.
[9] N.H. Ince, Ultrasound-assisted advanced oxidation processes for water decontamination, Ultrason. Sonochem. 40 (2018) 97–103. https://doi.org/10.1016/j.ultsonch.2017.04.009.
[10] P. Ritesh, V.C. Srivastava, Understanding of ultrasound enhanced electrochemical oxidation of persistent organic pollutants, J. Water Process Eng. 37 (2020) 101378. https://doi.org/10.1016/j.jwpe.2020.101378.
[11] G. Perez, A.R. Fernandez-Alba, A.M. Urtiaga, I. Ortiz, Electro-oxidation of reverse osmosis concentrates generated in tertiary water treatment, Water Res. 44 (2010) 2763–2772. https://doi.org/10.1016/j.watres.2010.02.017.
[12] Y. Lan, C. Coetsier, C. Causserand, K. Groenen Serrano, On the role of salts for the treatment of wastewaters containing pharmaceuticals by electrochemical oxidation using a boron doped diamond anode, Electrochimica Acta. 231 (2017) 309–318. https://doi.org/10.1016/j.electacta.2017.01.160.
[13] A.B. Rostam, M. Taghizadeh, Advanced oxidation processes integrated by membrane reactors and bioreactors for various wastewater treatments: A critical review, J. Environ. Chem. Eng. 8 (2020) 104566. https://doi.org/10.1016/j.jece.2020.104566.
[14] Y. Lan, L. Barthe, A. Antonin, C. Causserand, Feasibility of a heterogeneous Fenton membrane reactor containing a Fe-ZSM5 catalyst for pharmaceuticals degradation: Membrane fouling control and long-term stability, Sep. Purif. Technol. 231 (2020) 115920. https://doi.org/10.1016/j.seppur.2019.115920.
[15] L. Borea, V. Naddeo, M.S. Shalaby, T. Zarra, V. Belgiorno, H. Abdalla, A.M. Shaban, Wastewater treatment by membrane ultrafiltration enhanced with ultrasound: Effect of membrane flux and ultrasonic frequency, Ultrasonics. (n.d.). https://doi.org/10.1016/j.ultras.2017.06.013.
[16] S. Lee, H.K. Shon, S. Hong, Dewatering of activated sludge by forward osmosis (FO) with ultrasound for fouling control, Desalination. (n.d.). https://doi.org/10.1016/j.desal.2017.02.010.
[17] H. Kyllönen, P. Pirkonen, M. Nyström, J. Nuortila-Jokinen, A. Grönroos, Experimental aspects of ultrasonically enhanced cross-flow membrane filtration of industrial wastewater, Ultrason. Sonochem. 13 (2006) 295–302. https://doi.org/10.1016/j.ultsonch.2005.04.006.
[18] R.-S. Juang, K.-H. Lin, Flux recovery in the ultrafiltration of suspended solutions with ultrasound, J. Membr. Sci. 243 (2004) 115–124. https://doi.org/10.1016/j.memsci.2004.06.013.
[19] M.O. Lamminen, H.W. Walker, L.K. Weavers, Mechanisms and factors influencing the ultrasonic cleaning of particle-fouled ceramic membranes, J. Membr. Sci. 237 (2004) 213–223. https://doi.org/10.1016/j.memsci.2004.02.031.
[20] A.L. Ahmad, N.F.C. Lah, S. Ismail, B.S. Ooi, Membrane Antifouling Methods and Alternatives: Ultrasound Approach, Sep. Purif. Rev. 41 (2012) 318–346. https://doi.org/10.1080/15422119.2011.617804.
[21] Introduction to Applied Ultrasonics, in: Appl. Sonochemistry, John Wiley & Sons, Ltd, 2002: pp. 1–24. https://doi.org/10.1002/352760054X.ch1.
[22] K.K. Latt, T. Kobayashi, Ultrasound-membrane hybrid processes for enhancement of filtration properties, Ultrason. Sonochem. 13 (2006) 321–328. https://doi.org/10.1016/j.ultsonch.2005.05.002.

595 [23] Y. Zhu, R. Zhu, Y. Xi, J. Zhu, G. Zhu, H. He, Strategies for enhancing the
596 heterogeneous Fenton catalytic reactivity: A review, Appl. Catal. B Environ. 255 (2019)
597 117739. https://doi.org/10.1016/j.apcatb.2019.05.041.
598 [24] H. Tekin, O. Bilkay, S.S. Ataberk, T.H. Balta, I.H. Ceribasi, F.D. Sanin, F.B. Dilek, U.
599 Yetis, Use of Fenton oxidation to improve the biodegradability of a pharmaceutical
600 wastewater, J. Hazard. Mater. 136 (2006) 258–265.
601 https://doi.org/10.1016/j.jhazmat.2005.12.012.
602 [25] A. Rodríguez, G. Ovejero, J.L. Sotelo, M. Mestanza, J. García, Heterogeneous Fenton
603 Catalyst Supports Screening for Mono Azo Dye Degradation in Contaminated
604 Wastewaters, Ind. Eng. Chem. Res. 49 (2010) 498–505.
605 https://doi.org/10.1021/ie901212m.
606 [26] S. Shin, H. Yoon, J. Jang, Polymer-encapsulated iron oxide nanoparticles as highly
607 efficient Fenton catalysts, Catal. Commun. 10 (2008) 178–182.
608 https://doi.org/10.1016/j.catcom.2008.08.027.
609 [27] Y. Segura, F. Martínez, J.A. Melero, R. Molina, R. Chand, D.H. Bremner,
610 Enhancement of the advanced Fenton process (Fe0/H2O2) by ultrasound for the
611 mineralization of phenol, Appl. Catal. B Environ. 113–114 (2012) 100–106.
612 https://doi.org/10.1016/j.apcatb.2011.11.024.
613 [28] S. Aghapour Aktij, A. Taghipour, A. Rahimpour, A. Mollahosseini, A. Tiraferri, A
614 critical review on ultrasonic-assisted fouling control and cleaning of fouled membranes,
615 Ultrasonics. 108 (2020) 106228. https://doi.org/10.1016/j.ultras.2020.106228.
616 [29] I. Masselin, X. Chasseray, L. Durand-Bourlier, J.-M. Lainé, P.-Y. Syzaret, D.
617 Lemordant, Effect of sonication on polymeric membranes, J. Membr. Sci. 181 (2001) 213–
618 220. https://doi.org/10.1016/S0376-7388(00)00534-2.
619 [30] H.M. Kyllönen, P. Pirkonen, M. Nyström, Membrane filtration enhanced by ultrasound:
620 a review, Desalination. 181 (2005) 319–335. https://doi.org/10.1016/j.desal.2005.06.003.
621 [31] M.O. Lamminen, H.W. Walker, L.K. Weavers, Cleaning of particle-fouled membranes
622 during cross-flow filtration using an embedded ultrasonic transducer system, J. Membr.
623 Sci. 283 (2006) 225–232. https://doi.org/10.1016/j.memsci.2006.06.034.
624 [32] F. Reuter, S. Lauterborn, R. Mettin, W. Lauterborn, Membrane cleaning with
625 ultrasonically driven bubbles, Ultrason. Sonochem. 37 (2017) 542–560.
626 https://doi.org/10.1016/j.ultsonch.2016.12.012.
627 [33] T.G. Leighton, The Acoustic Bubble, Elsevier, 1994.
628 [34] A. Mirzaei, Z. Chen, F. Haghighat, L. Yerushalmi, Removal of pharmaceuticals from
629 water by homo/heterogonous Fenton-type processes – A review, Chemosphere. 174 (2017)
630 665–688. https://doi.org/10.1016/j.chemosphere.2017.02.019.
631 [35] N. Khatri, S. Tyagi, D. Rawtani, Recent strategies for the removal of iron from water:
632 A review, J. Water Process Eng. 19 (2017) 291–304.
633 https://doi.org/10.1016/j.jwpe.2017.08.015.
634 [36] O. Naji, R.A. Al-juboori, A. Khan, S. Yadav, A. Altaee, A. Alpatova, S. Soukane, N.
635 Ghaffour, Ultrasound-assisted membrane technologies for fouling control and performance
636 improvement: A review, J. Water Process Eng. 43 (2021) 102268.
637 https://doi.org/10.1016/j.jwpe.2021.102268.
638 [37] Y. Gu, C. Chen, J. Tu, X. Guo, H. Wu, D. Zhang, Harmonic responses and cavitation
639 activity of encapsulated microbubbles coupled with magnetic nanoparticles, Ultrason.
640 Sonochem. 29 (2016) 309–316. https://doi.org/10.1016/j.ultsonch.2015.10.006.
641 [38] V. Grosjean, C. Julcour, O. Louisnard, L. Barthe, Axial acoustic field along a solid-
642 liquid fluidized bed under power ultrasound, Ultrason. Sonochem. 56 (2019) 274–283.
643 https://doi.org/10.1016/j.ultsonch.2019.04.028.

[39] S. Adityosulindro, L. Barthe, K. González-Labrada, U. Javier Jáuregui Haza, H. Delmas, C. Julcour, Sonolysis and sono-Fenton oxidation for removal of ibuprofen in (waste)water, Ultrason. Sonochem. (n.d.). https://doi.org/10.1016/j.ultsonch.2017.06.008.
[40] C.Y. Tang, Y.-N. Kwon, J.O. Leckie, Effect of membrane chemistry and coating layer on physiochemical properties of thin film composite polyamide RO and NF membranes: I. FTIR and XPS characterization of polyamide and coating layer chemistry, Desalination. 242 (2009) 149–167. https://doi.org/10.1016/j.desal.2008.04.003.
[41] C. Causserand, S. Rouaix, J.-P. Lafaille, P. Aimar, Ageing of polysulfone membranes in contact with bleach solution: Role of radical oxidation and of some dissolved metal ions, Chem. Eng. Process. Process Intensif. 47 (2008) 48–56. https://doi.org/10.1016/j.cep.2007.08.013.
[42] A. Antony, A. Branch, G. Leslie, P. Le-Clech, Impact of membrane ageing on reverse osmosis performance – Implications on validation protocol, J. Membr. Sci. 520 (2016) 37–44. https://doi.org/10.1016/j.memsci.2016.07.036.
[43] R. Prulho, S. Therias, A. Rivaton, J.-L. Gardette, Ageing of polyethersulfone/polyvinylpyrrolidone blends in contact with bleach water, Polym. Degrad. Stab. 98 (2013) 1164–1172. https://doi.org/10.1016/j.polymdegradstab.2013.03.011.
[44] O.A. Makhotkina, E.V. Kuznetsova, S.V. Preis, Catalytic detoxification of 1,1-dimethylhydrazine aqueous solutions in heterogeneous Fenton system, Appl. Catal. B Environ. 68 (2006) 85–91. https://doi.org/10.1016/j.apcatb.2006.07.008.
[45] F. Velichkova, C. Julcour-Lebigue, B. Koumanova, H. Delmas, Heterogeneous Fenton oxidation of paracetamol using iron oxide (nano)particles, J. Environ. Chem. Eng. 1 (2013) 1214–1222. https://doi.org/10.1016/j.jece.2013.09.011.

669

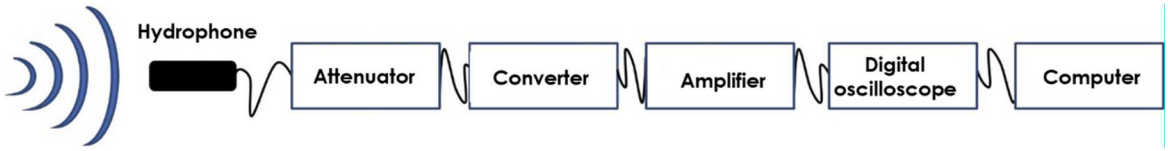

670

671 Figure 1: Pressure measurement system

672

673

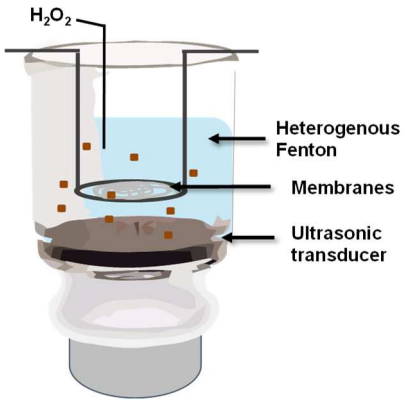

674

675 Figure 2: Membrane stability test set-up

676

677

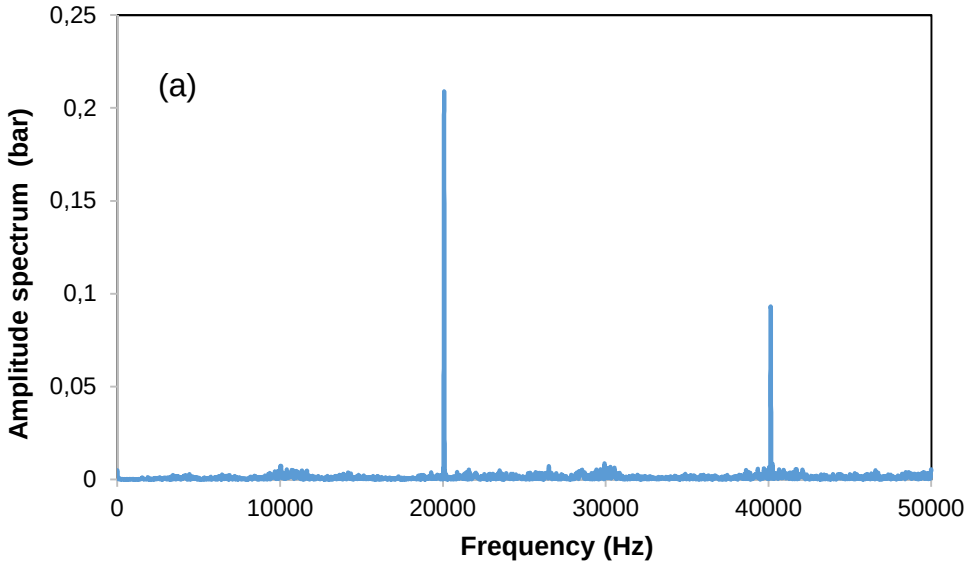
(a)
Amplitude spectrum (bar)
0,25
0,2
0,15
0,1
0,05
0
0
10000
20000
30000
40000
50000
Frequency (Hz)

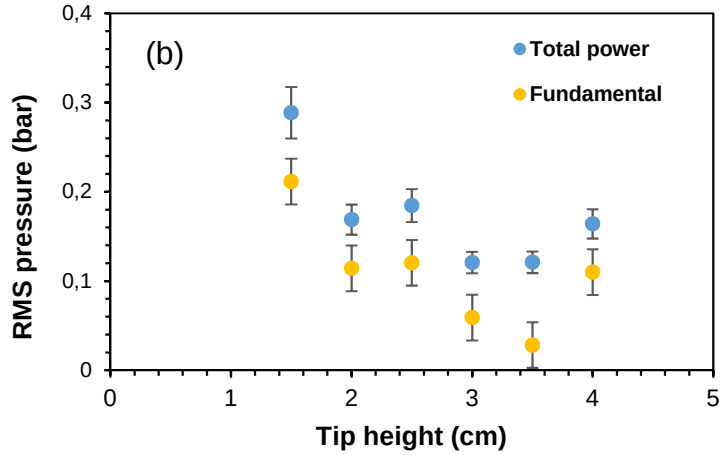
(b)
Total power
Fundamental
RMS pressure (bar)
0,4
0,3
0,2
0,1
0
0
1
2
3
4
5
Tip height (cm)

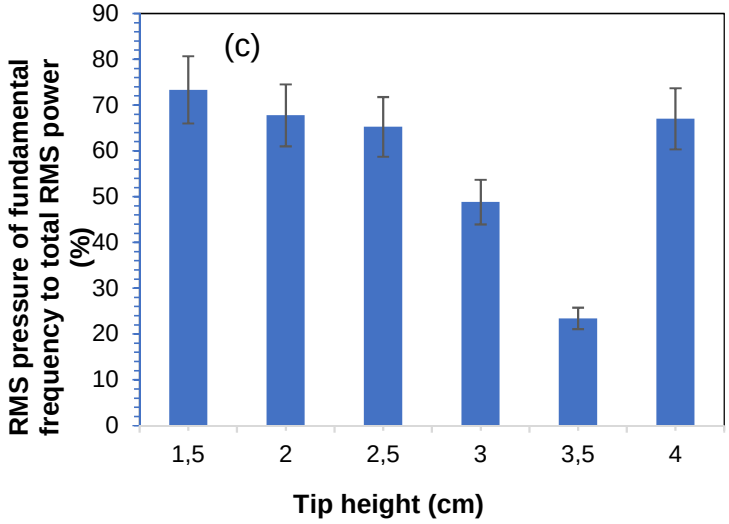
(c)
RMS pressure of fundamental frequency to total RMS power (%)
90
80
70
60
50
40
30
20
10
0
1,5
2
2,5
3
3,5
4
Tip height (cm)

678

679 Figure 3: Analysis of cavitation intensity: (a) ultrasonic wave spectrum at 1.5 cm tip
680 height (axial distance to the transducer tip); (b) RMS acoustic pressure of fundamental
681 frequency (20 kHz) and total power as function of tip height; (c) the ratio of RMS acoustic
682 pressure of fundamental frequency to total power.

683

684

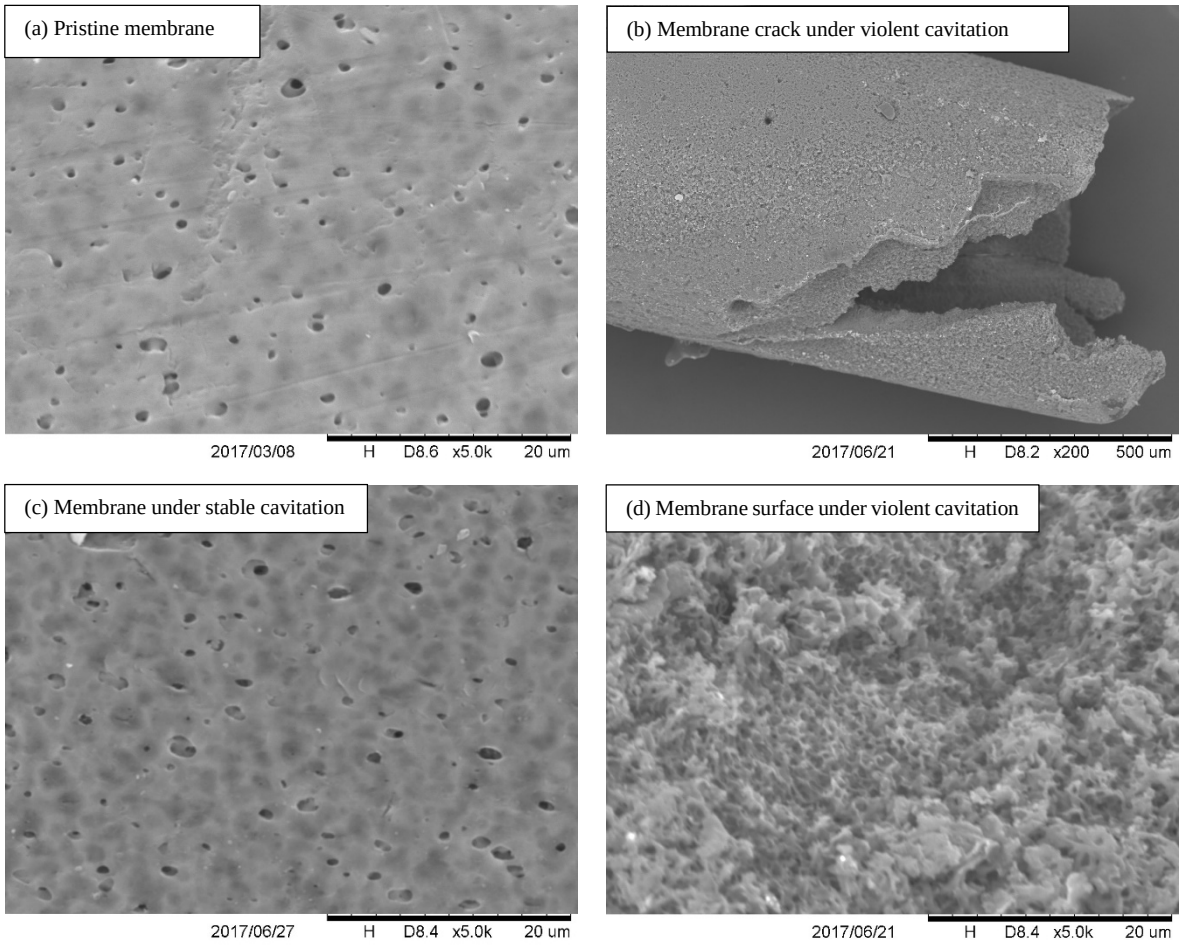

Figure 4: SEM images of (a) pristine membrane surface (×5000), and of membranes exposed to 10-hour continuous 50 W ultrasonic irradiation: (b) membrane crack section under violent cavitation (×200), (d) membrane surface under violent cavitation (×5000), (c) membrane surface under stable cavitation (×5000).

690

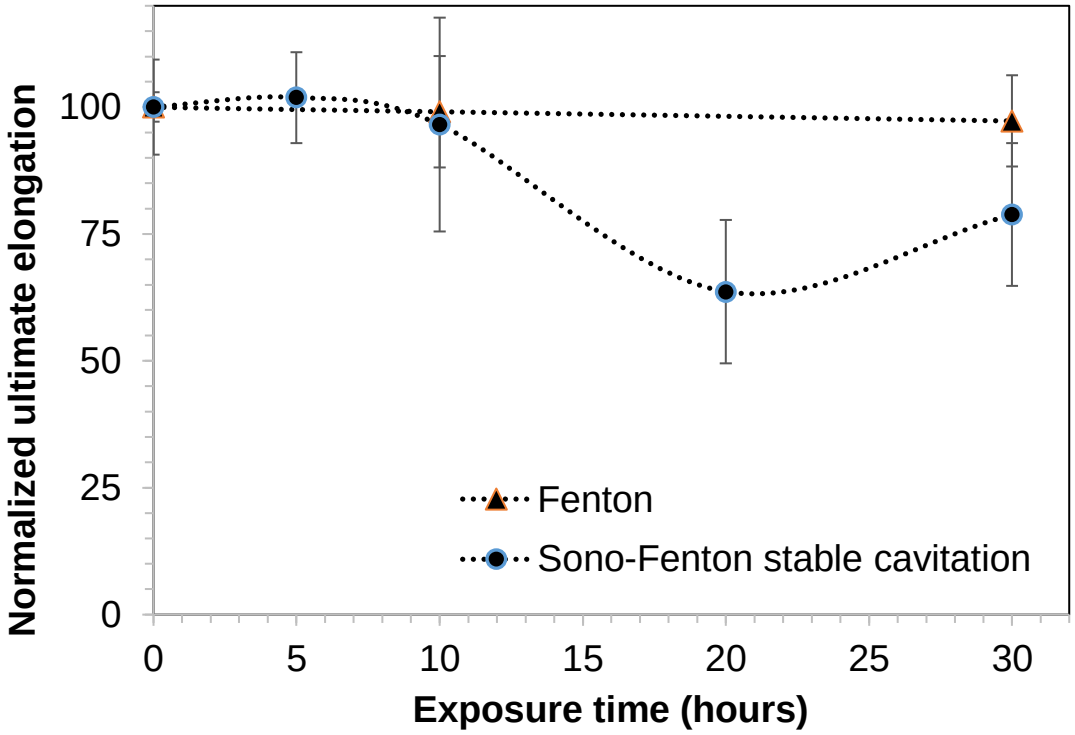
Normalized ultimate elongation
100
75
50
25
0
0
5
10
15
20
25
30
Exposure time (hours)
Fenton
Sono-Fenton stable cavitation

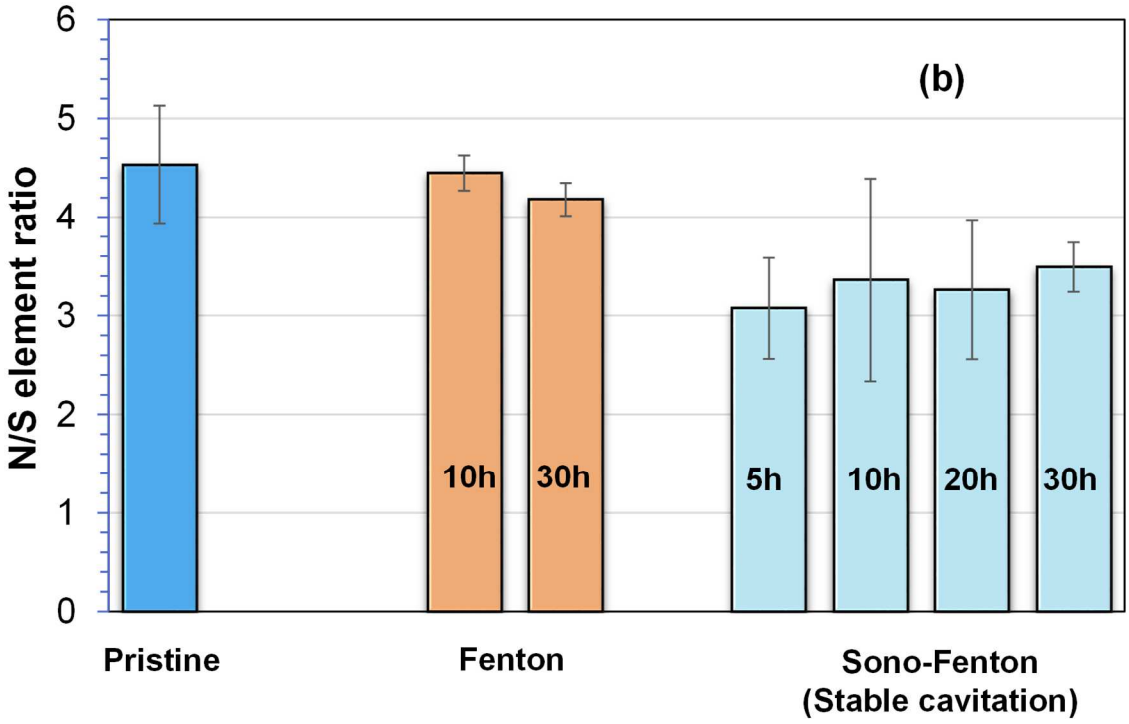
(b)
N/S element ratio
6
5
4
3
2
1
0
10h
30h
5h
10h
20h
30h
Pristine
Fenton
Sono-Fenton
(Stable cavitation)

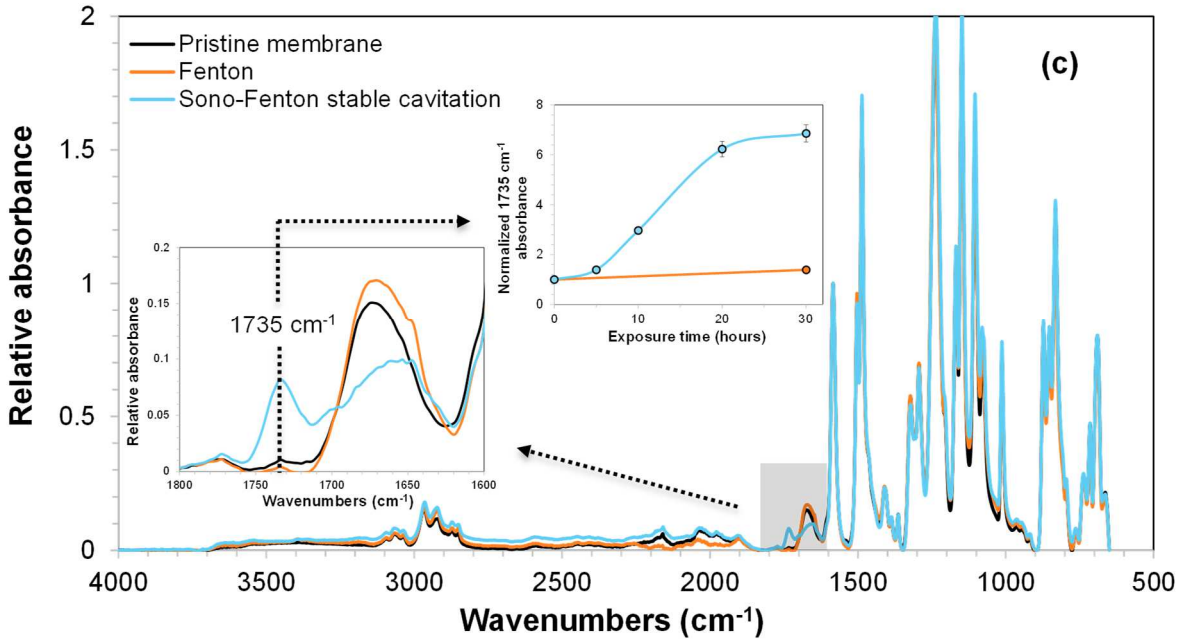

Figure 5: Characterization of pristine and aged membranes in Fenton and Sono-Fenton (stable cavitation region) conditions: (a) Ultimate elongation of membranes versus exposure time, (b) N/S elemental ratio, (c) FTIR spectrum and normalized relative FTIR absorbance at 1735 cm^{-1} (characteristic of non-cyclic imide groups, PVP chain scission products) against exposure time.

691

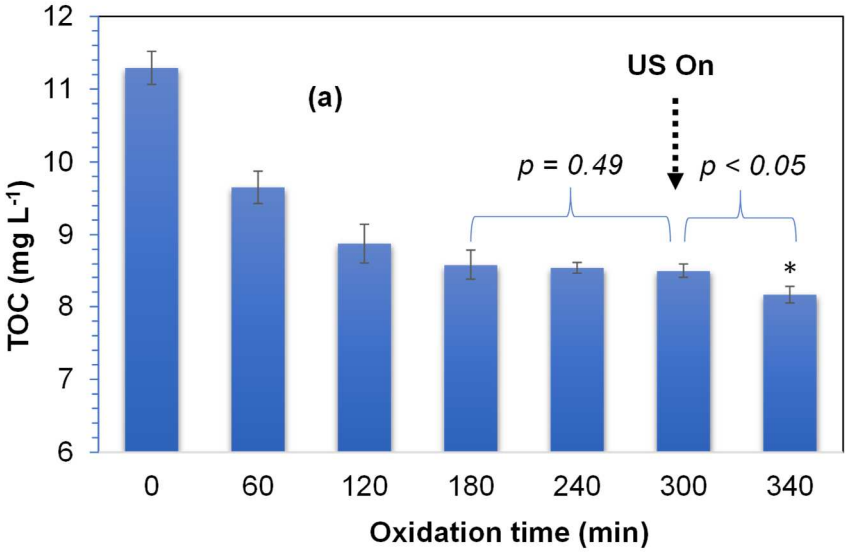
(a)
US On
p = 0.49
p < 0.05
*
TOC (mg L-1)
12
11
10
9
8
7
6
0
60
120
180
240
300
340
Oxidation time (min)

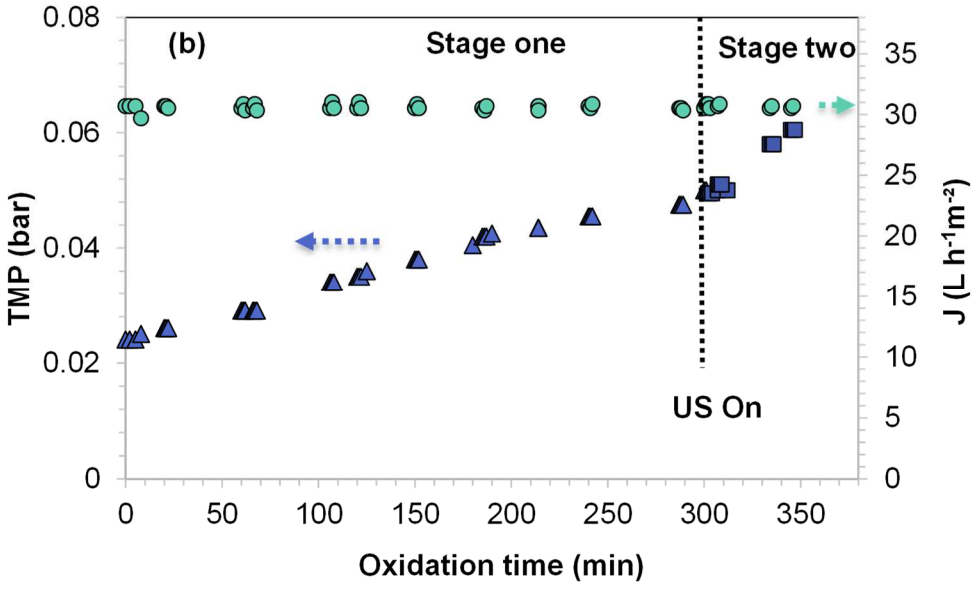
(b)
Stage one
Stage two
US On
TMP (bar)
J (L h-1m-2)
0.08
0.06
0.04
0.02
0
35
30
25
20
15
10
5
0
0
50
100
150
200
250
300
350
Oxidation time (min)

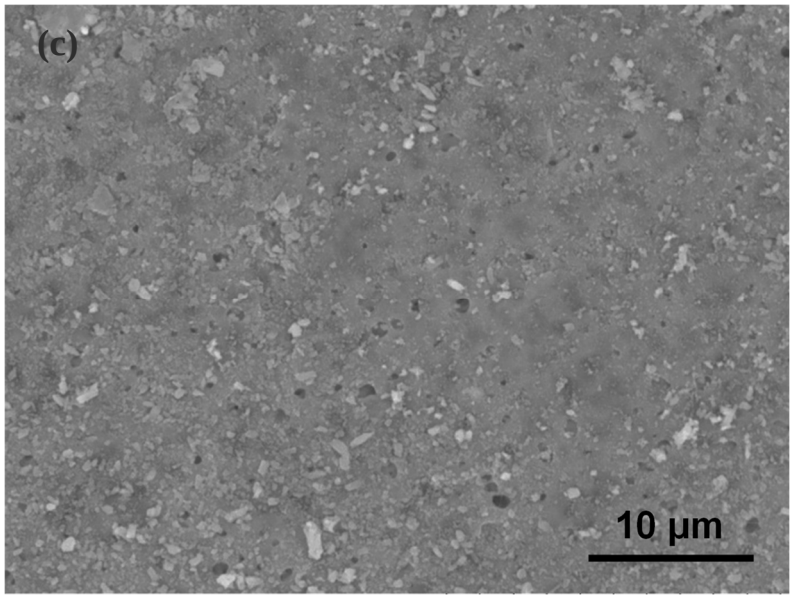
(c)
10 µm

Figure 6: HSoFM reactor performances with US off and on: (a) TOC over the experimental time (b) evolution of the transmembrane pressure of filtration, (c) SEM image of membranes at the end of filtration and oxidation (300 mins US off and 50 mins US on), the HSoFM reactor containing 4.8 g L^{-1} zeolite catalysts and H_2O_2 concentration maintained at 6.4 mM. (*) means statistical significance in comparison with control ($p < 0.05$)

692